IJIREEICE ISSN (O) 2321-2004, ISSN (P) 2321-5526

International Journal of Innovative Research in Electrical, Electronics, Instrumentation and Control Engineering

Impact Factor 8.021 ⁜ Peer-reviewed & Refereed journal ⁜ Vol. 14, Issue 7, July 2026

DOI: 10.17148/IJIREEICE.2026.14709

Detection of Peak Peripheral Blood Flow

Sabiha G. Shaikh[1], Uttam R. Bagal[1]

MGM's College of Engineering and Technology, Navi Mumbai, Maharashtra, India. 410206[1]

Abstract: Electrical impedance measurement of a body segment is performed by applying a low-amplitude, high frequency constant current through one pair of electrodes, while the resulting voltage is recorded using a separate pair of sensing electrodes. The measured voltage varies with the volume of blood present in the measured region. The negative first derivative of the impedance waveform is a peripheral blood flow (PBF) signal. Distinct fiducial points in the PBF waveform correspond to specific phases of the cardiac cycle, utilized to derive cardiovascular parameters and assess beat-to-beat variations. This study investigates automated detection of peaks in the PBF signal using three methods based on custom logic, implemented on PBF signals from subjects with normal health, hypertension, lung cancer, and coronary artery disease. Signals were recorded from 6 subjects of each type, yielding 24 recordings of 8,996 cycles. Method M3 achieved sensitivity 99.57%, precision 99.71%, F1-score 99.64%, and detection error 0.72%, outperforming all other methods.

Keywords: Electrical impedance, Fiducial points, Peripheral blood flow (PBF), Wavelet methods.

I. INTRODUCTION

Measurement of electrical impedance of a body segment involves injecting a constant current of low amplitude and high frequency using current-injecting electrodes and picking up the induced voltage using voltage-sensing electrodes. The demodulated voltage is proportional to variations in blood volume, called the impedance signal. The negative of the first derivative of the impedance signal is a peripheral blood flow (PBF) signal [1]. Landmarks in PBF are associated with different cardiac cycle events and are used for estimation of cardiovascular indices. Variations in electrical impedance at the periphery can be used to study hemodynamics and cardiovascular disorders [2]. A device for recording the PBF signal was validated clinically and reported effective across physiological and pathological conditions [7]– [9].

A typical PBF signal with its peak 'C' is shown in Fig. 1. The C peak corresponds to the point at which the impedance waveform changes most rapidly, associated with peak blood flow during ventricular ejection. It is used for cardiac-cycle segmentation, heart-rate variability (HRV) analysis, and vascular compliance estimation [21], [22]. Prior investigators incorporated ensemble averaging, adaptive filtering, wavelet denoising, and ECG synchronization to enhance C-point detection [1]– [6], [10], [26]– [29].

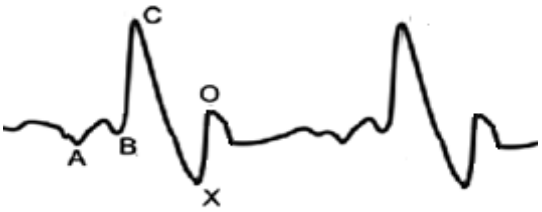

Fig. 1. Normal peripheral pulse waveform showing fiducial points A (onset), B (upstroke), C (systolic peak), X (dicrotic notch), and O (diastolic trough); y-axis: impedance change rate; x-axis: time.

Despite substantial progress, existing C-point detection methods remain less robust for heterogeneous, noisy, or pathological datasets [23]. To address this, three methods are proposed: (1) Fixed-Threshold, (2) Wavelet-Based Slope Assisted, and (3) Adaptive Threshold Wavelet-Enhanced Slope-Aided peak detection. Methods were implemented in MATLAB and evaluated using sensitivity, precision, detection error rate, and F1-score. The detected C-points were validated against manually annotated reference locations. Processed signals were used solely to facilitate peak detection, whereas final C-point localization was performed on the raw waveform to preserve physiological fidelity.

II. MATERIAL AND METHODS

A. Dataset

Peripheral pulse recordings were obtained from 24 subjects, including healthy individuals and subjects diagnosed with hypertension, coronary artery disease, and lung cancer. Signals were acquired at 500 samples/s with continuous five-

IJIREEICE ISSN (O) 2321-2004, ISSN (P) 2321-5526
International Journal of Innovative Research in Electrical, Electronics, Instrumentation and Control Engineering
Impact Factor 8.021 ⁜ Peer-reviewed & Refereed journal ⁜ Vol. 14, Issue 7, July 2026
DOI: 10.17148/IJIREEICE.2026.14709

minute recordings per subject. The dataset was curated by the Biomedical Engineering Department, MGM's College of Engineering and Technology, Navi Mumbai, and Father Muller Medical College & Hospital, Mangalore.

B. Proposed Methods for C-Point Detection

1) Method-1: Fixed-Threshold Peak Detection

The forward difference was scanned for peaks with amplitude exceeding an empirically chosen threshold of 120 units. Detected peaks are of two types: (i) a single local maximum exceeding the threshold, marked as the C peak; or (ii) multiple equal-amplitude peaks exceeding the threshold, where the midpoint is marked as the C peak. The algorithm is shown in Fig. 2.

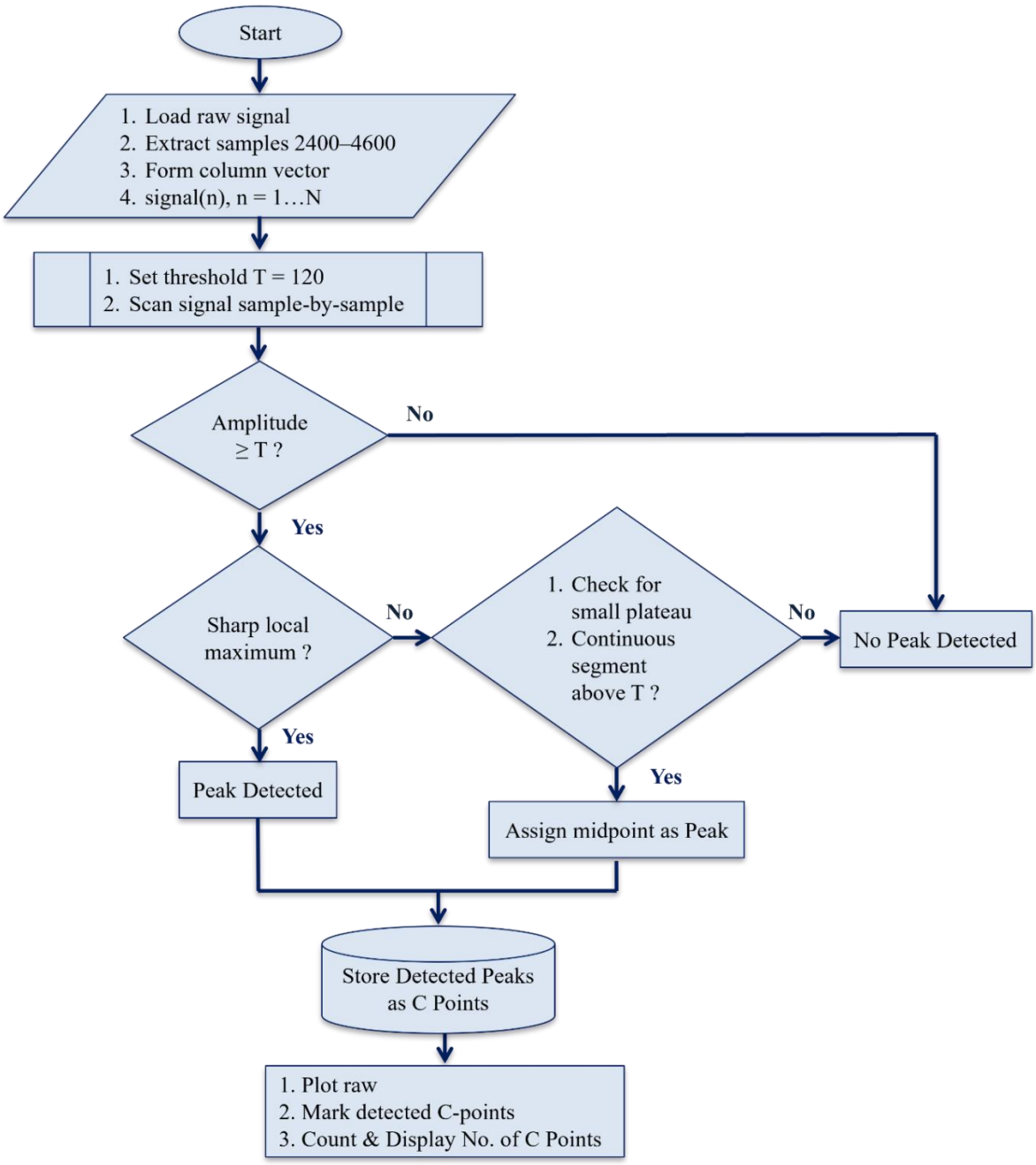

Fig. 2. Flowchart of Method 1 (Fixed-Threshold Peak Detection).

2) Method-2: Wavelet-Based Slope-Assisted Peak Detection

The raw signal segment (samples 2400–4600) was extracted at Fs = 500 Hz. A four-level Daubechies-4 (db4) wavelet decomposition was applied; detail coefficients D3 and D4 were reconstructed to extract high-frequency components, and

IJIREEICE ISSN (O) 2321-2004, ISSN (P) 2321-5526

International Journal of Innovative Research in Electrical, Electronics, Instrumentation and Control Engineering

Impact Factor 8.021 ⁜ Peer-reviewed & Refereed journal ⁜ Vol. 14, Issue 7, July 2026

DOI: 10.17148/IJIREEICE.2026.14709

the signal was normalized. The first derivative d1 = diff(signal) was computed to identify valid upstrokes. C-point detection was performed cycle-wise using 0.8 s windows with 0.5 s step. A ±6-sample refinement window retained candidates satisfying: (i) local maximum in original signal, and (ii) d1(i) > 0. A scoring function score = signal(i) × d1(i) selected the best candidate. Duplicate detections within 0.4 s were prevented. The algorithm is shown in Fig. 3.

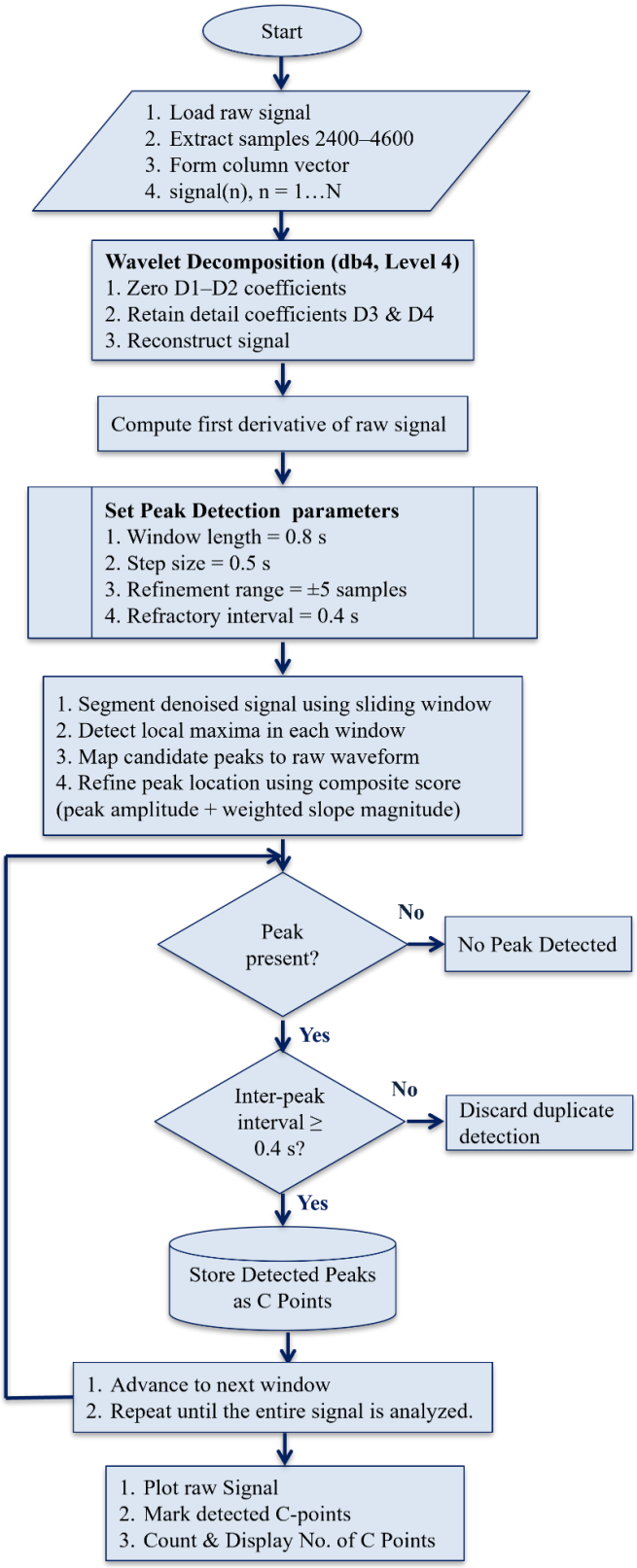

Fig. 3. Flowchart of Method 2 (Wavelet-Based Slope-Assisted Peak Detection).

IJIREEICE ISSN (O) 2321-2004, ISSN (P) 2321-5526

International Journal of Innovative Research in Electrical, Electronics, Instrumentation and Control Engineering

Impact Factor 8.021 ⁜ Peer-reviewed & Refereed journal ⁜ Vol. 14, Issue 7, July 2026

DOI: 10.17148/IJIREEICE.2026.14709

3) Method-3: Adaptive Threshold Wavelet-Enhanced Slope-Aided Peak Detection

After extraction, a zero-phase moving average filter (0.75 s window ≈ 375 samples) removed baseline drift: signal corrected = signal - baseline. Wavelet denoising using db4 at level 4 zeroed detail coefficients D1 and D2. Peak detection used MATLAB's findpeaks with adaptive threshold amp_thresh = mean(smoothed) + 0.4×std(smoothed) and minimum inter-peak distance of 0.35 s. Slope-based validation required the derivative to exceed 0.08×max(diff_sig) in a 100 ms pre-peak window. A final ±3 sample refinement corrected temporal shifts in the original signal. The algorithm is shown in Fig. 4.

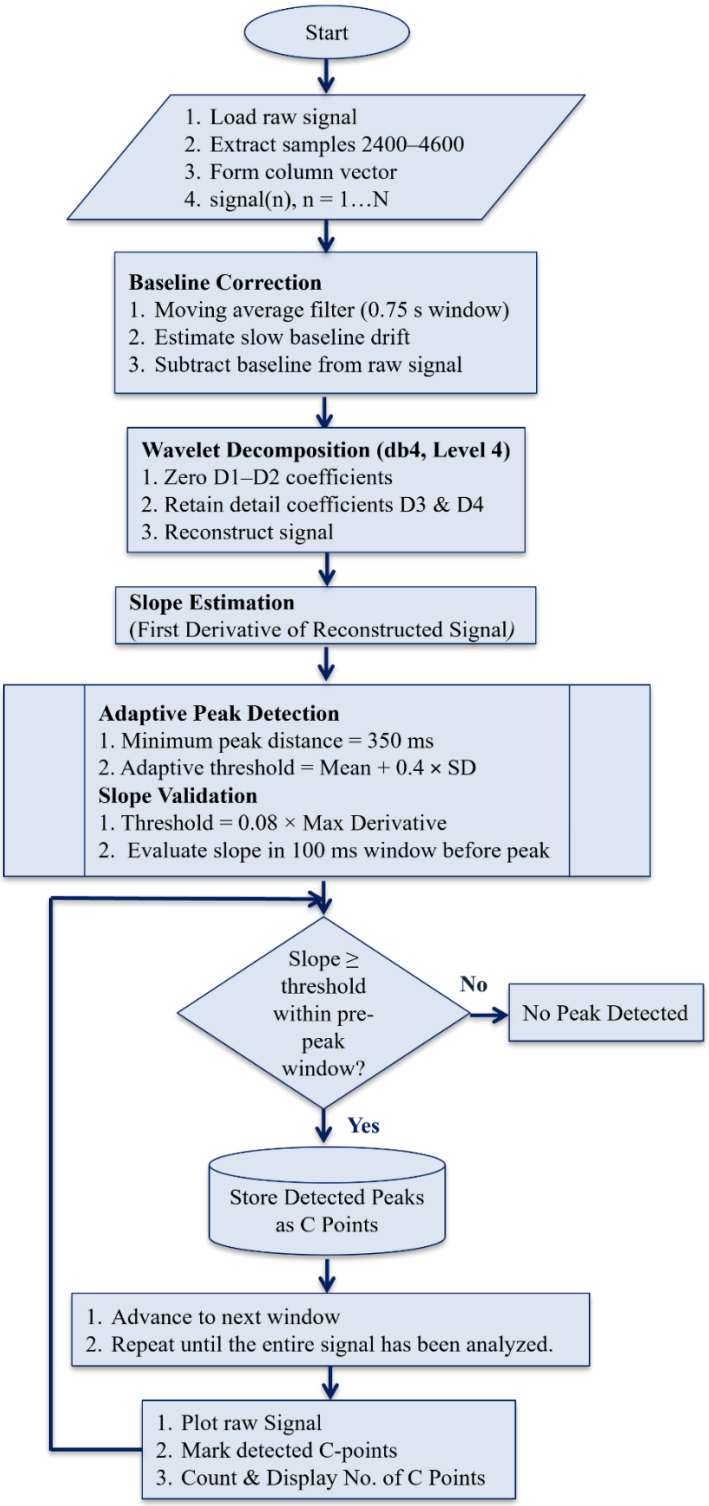

Fig. 4. Flowchart of Method 3 (Adaptive Threshold Wavelet Enhanced Slope-Aided Peak Detection).

IJIREEICE ISSN (O) 2321-2004, ISSN (P) 2321-5526

International Journal of Innovative Research in Electrical, Electronics, Instrumentation and Control Engineering

Impact Factor 8.021 ⁜ Peer-reviewed & Refereed journal ⁜ Vol. 14, Issue 7, July 2026

DOI: 10.17148/IJIREEICE.2026.14709

C. Evaluation Methods

The performance of each method was evaluated using the following metric definitions:

- TPC = Total C Points Detected (TCPD)– FPC, number of correctly detected C points.
- Sensitivity (Recall) $= \frac{\text{TPC}}{\text{TPC+FNC}} \times 100$, quantifying the proportion of physiologically valid C-points correctly identified.
- Precision (Positive Predictive Value, %) $= \frac{\text{TPC}}{\text{TP+FPC}} \times 100$, indicating the proportion of detected peaks that are true C-point.
- Detection Error Rate (%) $= \frac{\text{FPC+FNC}}{\text{TPC+FNC}} \times 100$ **,** measuring the relative incidence of misdetections.
- F1 Score (%) $= \frac{2(\text{Precision} \times \text{Sensitivity})}{\text{Precision+Sensitivity}}$, providing a harmonic mean of sensitivity and precision to capture overall detection reliability.

III. RESULTS AND DISCUSSION

Fig. 5 illustrates C-point detection for Subject AA (CAD) using M1–M3 (× markers). M1 over-detected peaks (13/6) with high false positives. M2 detected all expected peaks (6/6) but with localization inaccuracies. The proposed M3 accurately detected and precisely localized all true systolic peaks (6/6), demonstrating the robustness of the combined baseline correction, wavelet denoising, adaptive thresholding, and slope validation.

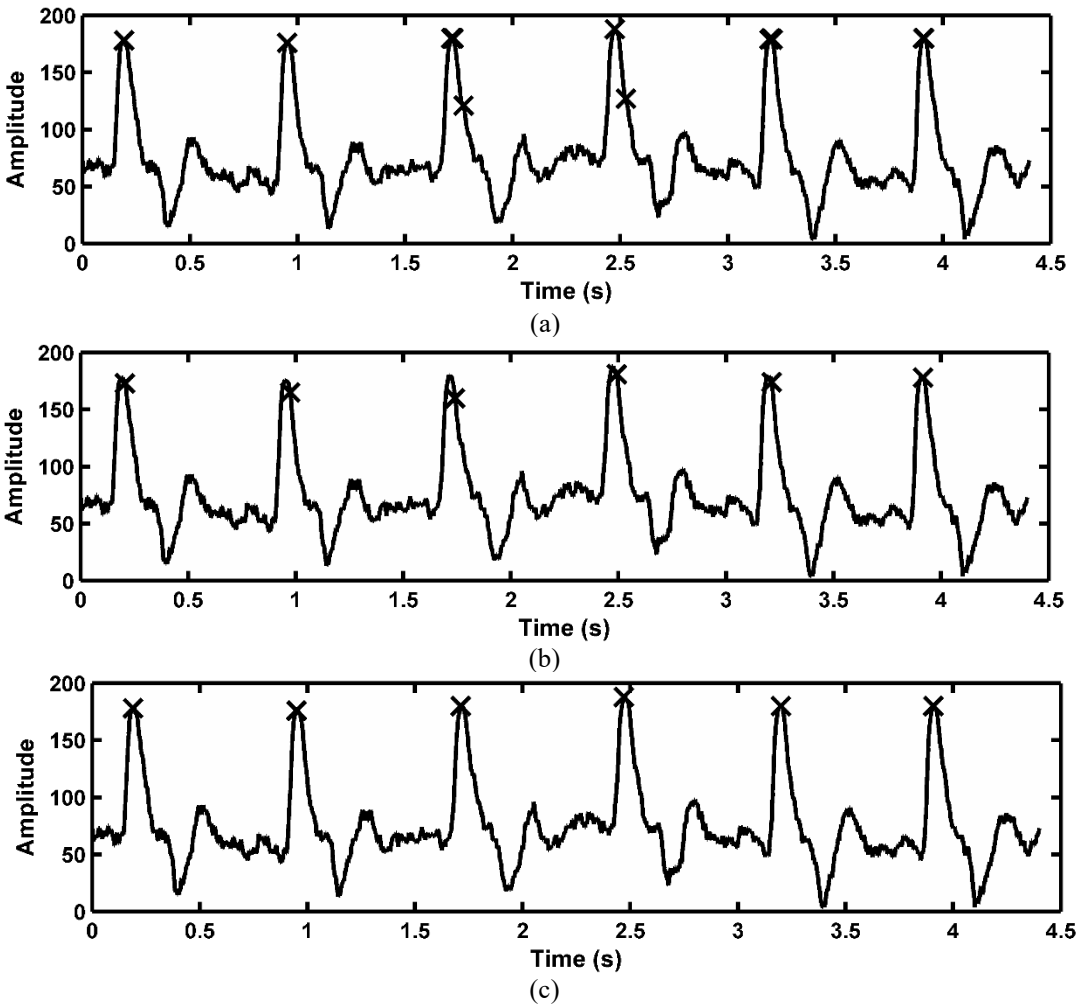

Fig. 5. Comparison of C-point detection methods M1, M2, and M3 (a, b, c) for Subject Code AA (CAD). Detected peak locations are marked by (×).

IJIREEICE ISSN (O) 2321-2004, ISSN (P) 2321-5526

International Journal of Innovative Research in Electrical, Electronics, Instrumentation and Control Engineering

Impact Factor 8.021 ⁜ Peer-reviewed & Refereed journal ⁜ Vol. 14, Issue 7, July 2026

DOI: 10.17148/IJIREEICE.2026.14709

TABLE I THE C PEAK DETECTION USING THE PROPOSED METHODS: M-1= METHOD-1, M2= METHOD-2, M3=METHOD-3. POINT COUNT: TCPD= TOTAL C POINTS DETECTED, TPC = TRUE POSITIVE COUNT, FPC = FALSE POSITIVE COUNT, FNC = FALSE NEGATIVE COUNT. RECORDING TYPE: SLC= SUBJECTS WITH LUNG CANCER, TOTAL CYCLES= *N*

Subject code (*n*)	Point count	Detection methods		
		Method-1	Method-2	Method-3
AU (415)	TCP	496	414	415
	TPC	413	348	415
	FPC	083	66	0
	FNC	002	67	0
AV (426)	TCP	381	424	426
	TPC	358	331	426
	FPC	023	93	0
	FNC	068	95	0
AW (428)	TCP	411	422	429
	TPC	300	347	427
	FPC	111	75	2
	FNC	128	81	1
AX (420)	TCP	409	419	419
	TPC	367	345	418
	FPC	42	74	1
	FNC	53	75	2
AZ (460)	TCP	99	429	450
	TPC	76	423	448
	FPC	23	6	2
	FNC	384	37	12
BA (516)	TCP	079	444	515
	TPC	078	422	514
	FPC	001	22	1
	FNC	438	94	1
Pooled (2665)	TCP	2075	2552	2654
	TPC	1603	2216	2648
	FPC	472	336	6
	FNC	1062	449	17

TABLE II THE C PEAK DETECTION USING THE PROPOSED METHODS: M-1= METHOD-1, M2= METHOD-2, M3=METHOD-3. POINT COUNT: TCPD= TOTAL C POINTS DETECTED, TPC = TRUE POSITIVE COUNT, FPC = FALSE POSITIVE COUNT, FNC = FALSE NEGATIVE COUNT. RECORDING TYPE: SUBJECTS WITH *CORONARY ARTERY DISEASE*, TOTAL CYCLES= *N*

Subject code (*n*)	Point count	Detection methods		
		Method-1	Method-2	Method-3
AA (354)	TCP	590	354	354
	TPC	319	291	354
	FPC	271	63	0
	FNC	35	63	0
AD (347)	TCP	611	347	347
	TPC	303	275	346
	FPC	308	72	1
	FNC	44	72	1
AF (307)	TCP	362	308	308
	TPC	234	263	307
	FPC	128	45	1
	FNC	73	44	0
AJ (281)	TCP	271	283	283
	TPC	227	177	281
	FPC	44	106	1
	FNC	54	104	0
AK (287)	TCP	256	289	289
	TPC	195	201	287
	FPC	61	88	2
	FNC	92	86	0
AQ (298)	TCPD	919	298	300
	TPC	267	229	298
	FPC	652	69	2
	FNC	31	69	0
Pooled (1874)	TCPD	3140	1879	1880
	TPC	1514	1582	1873
	FPC	1507	297	7
	FNC	360	292	1

IJIREEICE ISSN (O) 2321-2004, ISSN (P) 2321-5526

International Journal of Innovative Research in Electrical, Electronics, Instrumentation and Control Engineering

Impact Factor 8.021 ⁜ Peer-reviewed & Refereed journal ⁜ Vol. 14, Issue 7, July 2026

DOI: 10.17148/IJIREEICE.2026.14709

TABLE III THE C PEAK DETECTION USING THE PROPOSED METHODS: M-1= METHOD-1, M2= METHOD-2, M3=METHOD-3. POINT COUNT: TCPD= TOTAL C POINTS DETECTED, TPC = TRUE POSITIVE COUNT, FPC = FALSE POSITIVE COUNT, FNC = FALSE NEGATIVE COUNT. RECORDING TYPE: SUBJECTS WITH HYPERTENSION, TOTAL CYCLES= *N*

Subject code (*n*)	Point count	Detection methods		
		Method-1	Method-2	Method-3
BS (325)	TCPD	5	329	330
	TPC	5	301	325
	FPC	0	28	5
	FNC	320	24	0
BU (429)	TCPD	186	425	429
	TPC	186	374	429
	FPC	0	51	0
	FNC	243	55	0
BV (481)	TCPD	968	432	478
	TPC	391	385	477
	FPC	577	47	1
	FNC	90	96	4
BW (330)	TCPD	0	329	329
	TPC	0	325	328
	FPC	0	4	1
	FNC	330	5	2
BX (368)	TCPD	249	368	368
	TPC	228	330	367
	FPC	21	38	1
	FNC	140	38	1
BY (391)	TCPD	156	393	393
	TPC	156	352	390
	FPC	0	41	3
	FNC	235	39	1
Pooled (2324)	TCPD	1564	2276	2327
	TPC	966	2067	2316
	FPC	598	209	11
	FNC	1358	257	8

TABLE IV THE C PEAK DETECTION USING THE PROPOSED METHODS: M-1= METHOD-1, M2= METHOD-2, M3=METHOD-3. POINT COUNT: TCPD= TOTAL C POINTS DETECTED, TPC = TRUE POSITIVE COUNT, FPC = FALSE POSITIVE COUNT, FNC = FALSE NEGATIVE COUNT. RECORDING TYPE: SUBJECTS WITH NORMAL HEALTH, TOTAL CYCLES= *N*

Subject code (*n*)	Point count	Detection methods		
		Method-1	Method -2	Method -3
BL (394)	TCPD	835	393	394
	TPC	340	352	394
	FPC	495	41	0
	FNC	54	42	0
BM (294)	TCPD	244	295	295
	TPC	242	275	294
	FPC	2	20	1
	FNC	52	19	0
BO (371)	TCPD	915	370	370
	TPC	306	327	370
	FPC	609	43	0
	FNC	65	44	1
BP (409)	TCPD	409	406	409
	TPC	409	391	409
	FPC	0	15	0
	FNC	0	18	0
BQ (304)	TCPD	238	304	305
	TPC	238	286	304
	FPC	0	18	1
	FNC	66	18	0
BR (361)	TCPD	534	360	360
	TPC	322	314	360
	FPC	212	46	0
	FNC	39	47	1
Pooled (2133)	TCPD	3175	2128	2133
	TPC	1857	1945	2131
	FPC	1318	183	2
	FNC	276	188	2

Tables I–IV confirm the trends observed in Fig. 5. Method M1 is prone to over-detection (high FPC) and missed events (high FNC). Method M2 shows improved consistency but localization inaccuracies persist. Method M3 consistently achieves accurate and reliable C-point detection across all subject categories.

IJIREEICE ISSN (O) 2321-2004, ISSN (P) 2321-5526

International Journal of Innovative Research in Electrical, Electronics, Instrumentation and Control Engineering

Impact Factor 8.021 ⁜ Peer-reviewed & Refereed journal ⁜ Vol. 14, Issue 7, July 2026

DOI: 10.17148/IJIREEICE.2026.14709

TABLE V OVERALL POINT COUNT OBTAINED ACROSS ALL 24 SUBJECTS, *TOTAL CYCLES= 8996: TPC = TRUE POSITIVE COUNT, FPC = FALSE POSITIVE COUNT, FNC = FALSE NEGATIVE COUNT. THE VALUES ARE CONSOLIDATED FROM THE POOLED RESULTS OF TABLES 1–4.*

Point Count	Detection methods		
	Method-1	Method-2	Method-3
TPC	5937	7644	8957
FPC	3686	1191	26
FNC	3059	1352	39

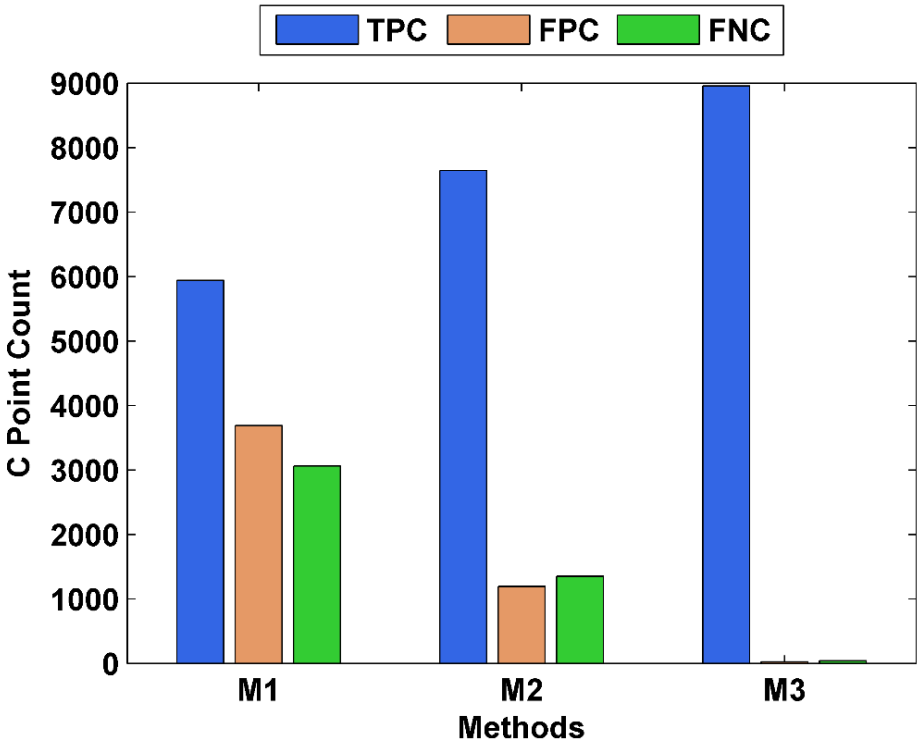

Fig. 6. Bar chart illustrating the distribution of TPC, FPC, and FNC counts for methods M1–M3, pooled across 24 subjects (8,996 cardiac cycles).

Table V and Fig. 6 present pooled results for all 24 subjects. The progressive improvement from M1 to M3 is evident, with M3 achieving the highest TPC and negligible false detections.

IJIREEICE ISSN (O) 2321-2004, ISSN (P) 2321-5526

International Journal of Innovative Research in Electrical, Electronics, Instrumentation and Control Engineering

Impact Factor 8.021 ⁜ Peer-reviewed & Refereed journal ⁜ Vol. 14, Issue 7, July 2026

DOI: 10.17148/IJIREEICE.2026.14709

TABLE VI C-PEAK DETECTION PERFORMANCE OF THE PROPOSED METHODS (M1–M3): *M1 = METHOD 1, M2 = METHOD 2, M3 = METHOD 3. PERFORMANCE METRICS INCLUDE SENSITIVITY (%), PRECISION (%), F1 SCORE (%) AND DETECTION ERROR RATE. THE TOTAL NUMBER OF ANALYSED CARDIAC CYCLES ANALYSED ARE 8996.*

Recording type (*n*)	Detection methods	Performance indices			
		Sensitivity	Precision	F1 score	Detection error rate
SNH (2133)	Method-1	87.06	58.49	69.97	74.73
	Method-2	91.19	91.40	91.29	17.39
	Method-3	99.91	99.91	99.91	0.19
SLC (2665)	Method-1	60.15	77.25	67.64	57.56
	Method-2	83.15	86.83	84.95	31.43
	Method-3	99.36	99.77	99.57	0.43
SCAD (1874)	Method-1	80.89	50.12	61.86	99.63
	Method-2	84.42	84.19	84.31	31.43
	Method-3	99.95	99.63	99.79	0.43
SHT (2324)	Method-1	41.57	61.76	49.69	84.17
	Method-2	88.94	90.82	89.87	20.05
	Method-3	99.66	99.53	99.59	0.82
Pooled (8996)	Method-1	65.99	61.70	63.77	74.98
	Method-2	84.97	86.52	85.74	28.27
	Method-3	99.57	99.71	99.64	0.72

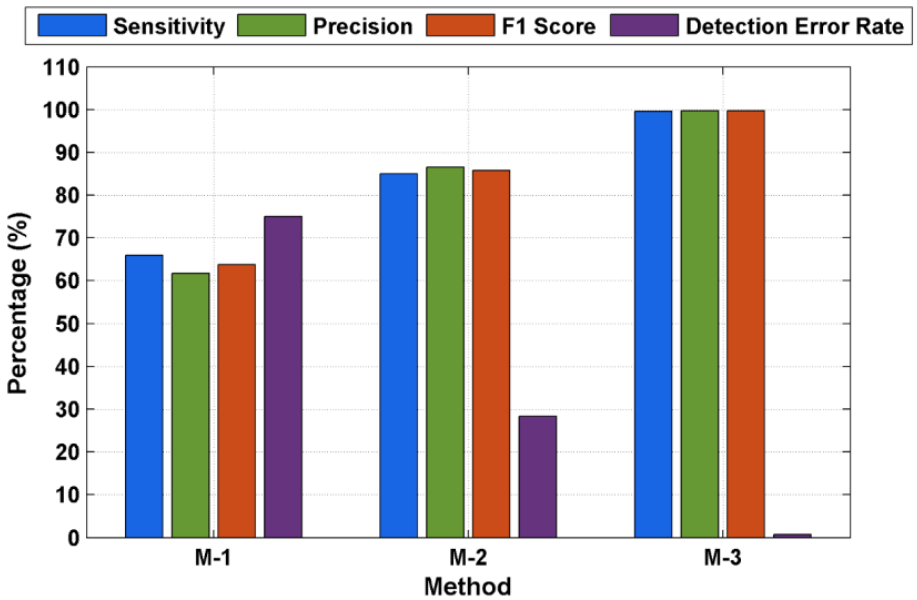

Fig. 7. Performance comparison of methods M1–M3: Sensitivity, Precision, F1-score, and Detection Error Rate.

Table VI and Fig. 7 confirms that M3 consistently outperforms M1 and M2, achieving high accuracy and minimal detection error across all recording types and subject categories.

DOI: 10.17148/IJIREEICE.2026.14709

IV. CONCLUSION

This study presented a comparative evaluation of three C-point detection methods for peripheral pulse waveforms derived from impedance plethysmography. Method M3 consistently achieved the best results, with high accuracy, strong robustness, and reliable performance across normal health, hypertension, lung cancer, and coronary artery disease. Its adaptive thresholding, wavelet-based denoising, and slope validation make it well-suited for clinical deployment across diverse physiological conditions.

ACKNOWLEDGMENT

The authors express their sincere gratitude to **Dr. Geeta S. Lathkar**, Director, and **Dr. V. G. Sayagavi**, Vice Principal, MGM's College of Engineering and Technology, for their valuable guidance, encouragement, and continuous support during this study.

REFERENCES

[1] J. Nyboer, M. M. Kreider, and L. Hannapel, "Electrical impedance plethysmography: A physical and physiologic approach to peripheral vascular study," Circulation, vol. 2, pp. 811–821, 1950.
[2] J. Nyboer, "Regional pulse volume and perfusion flow measurement: Electrical impedance plethysmography," AMA Arch. Internal Med., vol. 105, no. 2, pp. 264–276, 1960.
[3] J. Nyboer, M. Marchal, and M. T. Marchal, "Intrathoracic volemic events by tetrapolar electrical impedance detection," Amer. J. Roentgenol., vol. 98, no. 2, pp. 482–486, 1966.
[4] W. G. Kubicek, J. N. Karnegis, R. P. Patterson, D. A. Witsoe, and R. H. Mattson, "Development and evaluation of an impedance cardiac-output system," Aerospace Med., vol. 37, pp. 1208–1212, 1966.
[5] W. G. Kubicek, R. P. Patterson, and D. A. Witsoe, "Impedance cardiography as a noninvasive method of monitoring cardiac function," Ann. New York Acad. Sci., vol. 170, pp. 724–732, 1970.
[6] Z. Lababidi et al., "The first derivative thoracic impedance cardiogram," Circulation, vol. 41, no. 4, pp. 651–658, 1970.
[7] G. D. Jindal et al., "Early detection of coronary heart disease using peripheral pulse analyzer," BARC Newsletter, vol. 326, pp. 15–21, 2012.
[8] G. D. Jindal et al., "Harmonic analysis of peripheral pulse for screening subjects at high risk of diabetes," J. Med. Eng. Technol., vol. 41, no. 6, pp. 437–443, 2017.
[9] K. Y. Hsiao et al., "Peripheral pulse harmonic analysis and its clinical application: A systematic review," J. Traditional Complementary Med., vol. 14, no. 2, pp. 223–236, 2023.
[10] A. C. Guyton and J. E. Hall, Textbook of Medical Physiology, 11th ed. Philadelphia, PA: Elsevier Saunders, 2006.
[11] K. Tavakolian, "Seismocardiography: Past, present and future," in Proc. 36th Annu. Int. Conf. IEEE EMBC, Chicago, IL, Aug. 2014, pp. 4455–4459.
[12] M. Di Rienzo et al., "Seismocardiography: A new technique for monitoring cardiac mechanical function," J. Appl. Physiol., vol. 114, pp. 611–622, 2013.
[13] O. T. Inan et al., "Ballistocardiography and seismocardiography: A review of recent advances," IEEE J. Biomed. Health Inform., vol. 19, pp. 1414–1427, 2015.
[14] E. A. Haapala et al., "Arterial stiffness and cardiovascular risk: Emerging insights from bioimpedance pulse analysis," Atherosclerosis, vol. 335, pp. 10–19, 2021.
[15] A. Yamashina et al., "Validity, reproducibility, and clinical significance of noninvasive brachial-ankle pulse wave velocity measurement," Hypertens. Res., vol. 25, no. 3, pp. 359–364, 2002.
[16] S. M. M. Naidu, U. R. Bagal, P. C. Pandey, S. Hardas, and N. D. Khambete, "Detection of characteristic points of impedance cardiogram and validation using Doppler echocardiography," in Proc. Annu. IEEE India Conf. (INDICON), Pune, 2014, pp. 1–6.
[17] U. R. Bagal et al., "Detection of opening and closing of the aortic valve using impedance cardiography and its validation by echocardiography," vol. 4, no. 1, Nov. 2018.
[18] L. Y. Shyu, Y. S. Lin, C. P. Liu, and W. C. Hu, "Detection of impedance-cardiogram characteristic points using wavelet transform," Comput. Biol. Med., vol. 34, pp. 165–175, 2004.
[19] M. Rizzi, M. D'Aloia, and B. Castagnolo, "High-sensitivity method to detect impedance-cardiography characteristic points using wavelet transform," J. Appl. Sci., vol. 9, pp. 1412–1421, 2009.
[20] S. Zhao et al., "Detection of impedance-cardiography characteristic points based on wavelet transform," in Proc. 27th Annu. Int. Conf. IEEE EMBC, Shanghai, 2005, pp. 2730–2732.

DOI: 10.17148/IJIREEICE.2026.14709

[21] A. P. DeMarzo and R. M. Lang, "A new algorithm for improved detection of aortic-valve opening by impedance cardiography," in Proc. Computers in Cardiology, Indianapolis, 1996, pp. 373–376.

[22] X. Hu, X. Chen, R. Ren, and Y. Wang, "Adaptive filtering and characteristic-extraction for impedance cardiography," J. Fiber Bioeng. Inform., vol. 7, pp. 81–90, 2014.

[23] M. Muzi, D. C. Jeutter, and J. J. Smith, "Computer-automated impedance-derived cardiac indexes," IEEE Trans. Biomed. Eng., vol. 33, pp. 42–47, 1986.

[24] Y. Zhang, M. Qu, J. G. Webster, W. J. Tompkins, B. A. Ward, and D. Bassett, "Cardiac output monitoring by impedance cardiography during treadmill exercise," IEEE Trans. Biomed. Eng., vol. BME-33, pp. 1037–1042, 1986.

[25] D. W. Kim, "Detection of physiological events by impedance," Yonsei Med. J., vol. 30, pp. 1–11, 1989.

[26] T. Sebastian, P. C. Pandey, S. M. M. Naidu, and V. K. Pandey, "Wavelet-based denoising for suppression of respiratory and motion artifacts in impedance cardiography," in Proc. Computers in Cardiology, Hangzhou, 2011, Paper P83.141.

[27] S. M. M. Naidu, P. C. Pandey, and V. K. Pandey, "Automatic detection of characteristic points in impedance cardiogram," in Proc. Computing in Cardiology, 2011, pp. 497–500.

[28] D. Lapsa et al., "PPG and bioimpedance-based wearable applications in heart rate monitoring—A comprehensive review," Appl. Sci., vol. 14, no. 17, p. 7451, 2024.

[29] R. Jain, A. Shah, and A. Jadhav, "Impedance plethysmography," in A Handbook on Physiological Variability, G. D. Jindal et al., Eds. Mumbai: Electronics Division BARC, 2010, pp. 34–39.

[30] D. Benitez et al., "The use of the Hilbert transforms in ECG signal analysis," Comput. Biol. Med., vol. 31, pp. 399–406, 2001.

[31] P. Carvalho et al., "Robust characteristic points for ICG: Definition and comparative analysis," in Proc. BIOSIGNALS, Rome, 2011, pp. 161–168.

[32] I. Karpiel et al., "An effective method of detecting characteristic points of impedance cardiogram verified in the clinical pilot study," Sensors, vol. 22, no. 24, p. 9872, 2022.

[33] I. B. Salah and K. Ouni, "Denoising of the impedance cardiography signal (ICG) for best detection of the characteristic points," in Proc. BioSMART 2017, Nov. 2017.

[34] U. Pale, N. Müller, A. Arza, and D. Atienza, "ReBeatICG: Real-time low-complexity beat-to-beat impedance cardiogram delineation algorithm," in Proc. 43rd Annu. Int. Conf. IEEE EMBC, Mexico, 2021, pp. 5618–5624.